

Theoretical study of the radiationless decay channels of triplet state norbornene

Stefan Grimme ^a, Markus Woeller ^a, Sigrid D. Peyerimhoff ^a, David Danovich ^b,
Sason Shaik ^b

^a *Institut für Physikalische und Theoretische Chemie der Universität Bonn, Wegelerstraße 12, 53115 Bonn, Germany*

^b *Department of Organic Chemistry and the Lise-Meitner-Minerva Centre for Computational Quantum Chemistry, The Hebrew University 91904, Jerusalem, Israel*

Received 24 November 1997; in final form 12 February 1998

Abstract

Four possible radiationless decay channels for the lowest triplet state (T_1) of norbornene to the singlet ground state (S_0) have been investigated by ab initio CASSCF, MRD-CI and unrestricted density functional calculations. Neither breaking a single bond, yielding a triplet biradical with an allylic substructure, nor pyramidalization of the double bond, was found to be an energetically reasonable decay pathway. All theoretical models agree that twisting around the double bond is the most favourable decay coordinate. Spin-orbit coupling matrix elements employing the CASSCF method are small ($0.5\text{--}1.5\text{ cm}^{-1}$) however, so the results for the gas-phase reaction do not support the short lifetime observed for the T_1 state in benzene solution, but show an interesting mechanism for decay in rigid systems. © 1998 Elsevier Science B.V. All rights reserved.

1. Introduction

A widespread and useful concept in organic photochemistry is the so-called ‘loose-bolt’ effect. Bridged and therefore rigid derivatives of unsaturated molecules (e.g. alkenes, stilbenes) usually exhibit longer lifetimes for the lowest excited singlet and triplet states (S_1 and T_1), larger emission quantum yields and a lower photochemical reactivity than the parent compounds [1]. This may be explained by the fact that relaxation modes on excited state hyper-surfaces are hindered by the strain introduced in the bridging moieties. Thus, avoided crossings of potential energy surfaces, photochemical funnels or points with energetic near degeneracy to other states are not reached on low energy pathways.

Norbornene, the simplest bicyclic alkene (see Fig. 1), seems not to follow this general trend. The experimental pulse-radiolysis/energy transfer study of Barwise et al [2] has shown that the non-emissive lowest triplet state has a lifetime of 250 ns in benzene solution at room temperature. From the experiments it was not clear if this value is near to the natural lifetime or if collision induced quenching with the solvent contributes significantly to the decay rate.

Comparison with the T_1 lifetimes of other alkenes in solution shows that the decay rate of norbornene is fast for a spin-forbidden $T_1 \rightarrow S_0$ transition from an unperturbed double bond geometry. For example, 1-phenylcyclobutene, which also has a quite rigid double bond geometry, exhibits a T_1 lifetime of 3.6

ms which decreases to only 160 μ s in 1-phenylcyclohexene [3] (i.e. due to a ‘loose-bolt’ effect).

For ethene it is well established that the lowest triplet state with a valence $\pi \rightarrow \pi^*$ electronic configuration has a minimum energy at a double bond twisting angle of 90 degrees, where it is nearly isoenergetic with the S_0 state, thus providing from energetic grounds the possibility for efficient $T_1 \rightarrow S_0$ radiationless decay. At first sight, however, this pathway seems unlikely in norbornene because the molecular framework with a *cis* configuration imposes limitations on the degree of twisting around the double bond. Therefore, other modes of relaxation, e.g. by syn-pyramidalization as well as biradical pathways ought to be considered.

In this Letter we try to gain insight into the experimental findings by performing ab initio complete active space self-consistent field (CASSCF) and unrestricted density functional calculations (UDFT) with full geometry optimization for norbornene. Four possible reactions pathways for $T_1 \rightarrow S_0$ radiationless decay were considered: I) breaking

of a single bond between C6 and C7, II) breaking of a single bond between C5 and C6, III) twisting around the CC double bond (dihedral angle C6–C1–C2–C3, θ_1 , see Fig. 1) and IV) pyramidalization of the two double bond carbon atoms in the same direction (i.e. retaining C_s symmetry; the relevant dihedral angles are θ_2 (H–C1–C2–C3) and θ_3 (H–C2–C1–C6).

Initial investigations with semiempirical MO methods indicated that of all the possible biradical mechanisms, the alternatives I) and II) are energetically most promising. Therefore, the CASSCF and UDFT studies were limited to these two pathways.

2. Theoretical methods

Ab initio CASSCF(n,m) calculations (active full CI space with n electrons in m orbitals) for the geometries and energetics of norbornene were performed with the MOLPRO [4] suite of programs. The TURBOMOLE codes [5,6] have been employed

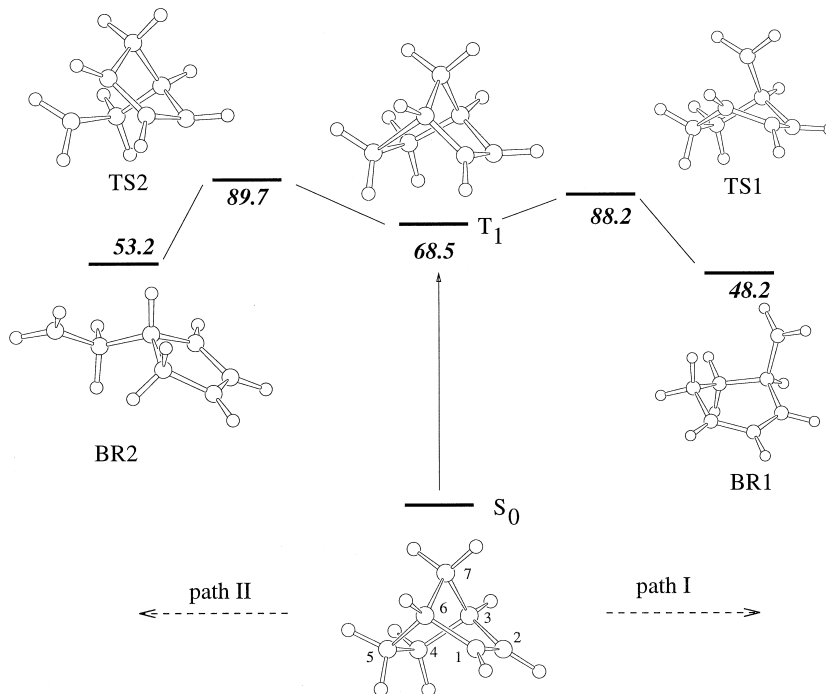


Fig. 1. Schematic energy diagram (energies relative to the S_0 state in kcal/mol) for the bond breaking reactions at the UDFT–B3LYP/SV + d level.

for the unrestricted density functional calculations (UDFT) with Becke's B3LYP hybrid exchange-correlation functional [7,8]. The Gaussian basis sets used are of split-valence quality (SV, [3s2p]/[2s] for C and H, respectively) [9] subsequently augmented with polarization d-functions at the carbon atoms ($\alpha_d = 0.8$, SV + d basis). All minima (on S_0 and T_1) and saddlepoints (T_1) were fully optimized with the eigenvector-following algorithm of Baker [10] without any symmetry constraints. The transition state structures were characterized as one-dimensional saddlepoints (one imaginary vibrational frequency) by force calculations at the semiempirical UPM3 [11] level. The pathways for double bond twisting and pyramidalization were investigated by choosing the dihedral angles Θ_1 and $\Theta_2 = -\Theta_3$, respectively, as reaction coordinates while optimizing all remaining geometric variables. In order to check the reliability of the UDFT and CASSCF results for the twisting potential curves we have performed multi-reference singles and doubles configuration interaction calculations (MRD-CI) [12–14] for the S_0 and T_1 states at several DFT optimized geometries. The optimized DFT geometries have been employed in these calculations which include the distribution of 38 valence electrons (the seven 1s core MOs were always doubly occupied) in 81 HF-SCF/SV + d MOs (the 30 highest lying virtual orbitals were discarded). For the S_0 state the total MRD-CI space consists of about 7.2×10^5 spin-adapted configurations state functions (CSF) from which 2×10^5 were treated variationally (energy section threshold $T = 0.5 \mu E_h$). The total MRD-CI spaces for the T_1 states were about 1.5×10^7 CSF from which $1.3\text{--}1.8 \times 10^6$ were selected at $T = 0.1 \mu E_h$. The reported CI energies include an extrapolation to $T = 0$ evaluated in the standard manner [12,13] and correspond to an estimated full CI according to a multireference analogue of the Davidson correction [15].

Spin-orbit coupling (SOC) calculations were done using the GAMESS [16] package which employs an approximate one-electron SO operator with an effective nuclear charge $Z^* = 3.6$, previously determined by Koseki and co-workers [17,18]. The SO calculations were carried out with CASSCF(n,m) wavefunctions. At the lowest level we used a minimal CASSCF(2,2) wavefunction which includes only the π and π^* orbitals, while the highest level involved

a CASSCF(10,10) calculation, where the ten orbitals are those which possess the largest coefficients on the double bond. A test near the S_0 – T_1 crossing point along the twist mode shows, that the calculated SOC value changes little when the active orbital space was varied from (8,8) to (10,10). Therefore, Table 2 only includes the SOC results for the (2,2) and (10,10) calculations. Full SO calculations with the Breit–Pauli (BP) operator were also carried out with GAMESS using a minimal CASSCF(2,2) wavefunction for the S_0 and T_1 states.

3. Results and discussion

The lowest theoretical levels for a description of the open-shell species ($^3\pi\pi^*$ and 3 biradicals) considered here are CASSCF wavefunctions with two active orbitals and the unrestricted self-consistent field approach. Due to the formation of an allylic substructure in the biradicals after the single bond breaking processes (BR1 [breaking C6–C7] and BR2 [breaking C5–C6], see Fig. 1) we have also performed CASSCF(4,4) calculations. The results differ only marginally from the CASSCF(2,2) data and are therefore not discussed further. In order to account for dynamical electron correlation and to reduce spin-contamination we have furthermore performed unrestricted calculations at the density functional level (UDFT–B3LYP). The results for geometries and relative energies are quite similar to the CASSCF data so that for the bond breaking processes only UDFT–B3LYP data will be presented.

The S_0 geometry of norbornene is found to possess C_s symmetry as expected (see Fig. 1 and Table 1): a planar C–C=C–C unit with a typical double bond length of 1.34 Å and a bicyclo[1.0.0]hexane moiety with CC single bond lengths of 1.52–1.57 Å. The vinylic hydrogens lie slightly below the C=C–C plane, i.e. the dihedral angles Θ_1 and Θ_2 , measuring this syn-pyramidalization, are -173.2 and 173.2 degrees, respectively. However, the resulting double-minimum potential (see below) has a low barrier of ≈ 1.2 kcal/mol which may not be present at higher theoretical levels.

In the T_1 state the C1–C2 bond is strongly elongated to 1.51 Å and a strong anti-pyramidalization of the hydrogen atoms at C1 and C2 ($\Theta_2 = -128.2$ and

Table 1

Optimized CC bond lengths, double bond twisting and pyramidalization angles Θ , total energies and \hat{S}^2 expectation values for the optimized S_0 and T_1 states and the stationary points along the bond breaking paths of norbornene at the UDFT–B3LYP/SV + d level

	State					
	S_0	T_1	TS_1	BR_1	TS_2	BR_2
$r(C1-C2) / \text{\AA}$	1.344	1.508	1.484	1.393	1.501	1.393
$r(C2-C3) / \text{\AA}$	1.523	1.514	1.508	1.512	1.524	1.513
$r(C3-C4) / \text{\AA}$	1.569	1.563	1.557	1.551	1.550	1.546
$r(C4-C5) / \text{\AA}$	1.562	1.565	1.558	1.538	1.526	1.493
$r(C5-C6) / \text{\AA}$	1.568	1.552	1.529	1.504	2.134	4.545
$r(C6-C1) / \text{\AA}$	1.523	1.517	1.403	1.393	1.390	1.393
$r(C6-C7) / \text{\AA}$	1.548	1.566	2.120	3.736	1.529	1.508
$r(C3-C7) / \text{\AA}$	1.548	1.549	1.514	1.505	1.559	1.565
$\Theta_1^a / \text{degrees}$	0.0	11.8	17.4	0.0	–9.5	0.0
$\Theta_2^b / \text{degrees}$	–173.2	–128.2	–142.0	177.3	131.8	179.2
$\Theta_3^c / \text{degrees}$	173.2	–121.3	–130.8	–179.1	154.1	–179.6
total energy / E_h	–272.31955	–272.21042	–272.17892	–272.24267	–272.17667	–272.23479
$\langle \hat{S}^2 \rangle^d$	0.0000	2.0046	2.0236	2.0337	2.0233	2.0319

^a Dihedral angle C6–C1–C2–C3.

^b Dihedral angle H–C1–C2–C3.

^c Dihedral angle H–C2–C1–C6.

^d $\langle \hat{S}^2 \rangle = 2$ is expected for a pure triplet state.

$\Theta_3 = -121.3$ degrees) is found. The C6–C1–C2–C3 twisting angle Θ_1 , however, is only 11.8 degrees which shows the rigidity of the norbornene skeleton. A second T_1 minimum with syn-pyramidalization (similar to the ground state) has been found to lie 3–4 kcal/mol higher in energy (see discussion below). The UDFT calculated adiabatic T_1 energy of 68.5 kcal/mol (24000 cm^{-1}) seems to be realistic. The experimental estimates are in the range 20000–25000 cm^{-1} [2]. Large scale CI calculations for ethene [19] yield a value of 64 kcal/mol which is nicely reproduced by UDFT–B3LYP (63.4 kcal/mol). The destabilization of the norbornene T_1 state relative to the corresponding ethene state derives from the marginal relaxation along the twisting coordinate imposed by the rigid bicyclic structure.

Transition state searches along the single bond breaking processes I) (C6–C7) and II) (C5–C6) in the excited triplet state have been successfully performed starting with hand-made initial guess geometries and numerical second derivatives (hessian matrix) from semiempirical UPM3 calculations. The structures of the transition states and the corresponding products (biradicals BR1 and BR2) found are

shown in Fig. 1 and some information about the geometrical parameters is compiled in Table 1. The broken CC bonds are elongated in TS1 and TS2 to ≈ 2.1 Å. The formation of allylic substructures in BR1 and BR2 (and to a smaller extent in TS1 and TS2) is deduced from the typical lengths of 1.39 Å for the C1–C2 and C6–C1 bonds. Although both triplet reactions are exothermic with respect to BR1 and BR2 by 20.3 and 15.3 kcal/mol, respectively, the computed barriers are high (19.7 and 21.2 kcal/mol). The higher stability of BR1 with respect to BR2 can be explained with the near strain free six-membered ring formed by reaction I), while path II) yields a structure with a five-membered ring. Assuming a ‘normal’ pre-exponential factor in Arrhenius law of 10^{10} – 10^{12} s^{-1} and taking the calculated barriers as activation energies we conclude that the two bond breaking processes are much too slow to explain the experimental T_1 lifetime of 250 ns. In this sense we estimate that any activated process on the T_1 surface has to occur with a barrier of less than 5 kcal/mol to account for the observed lifetime [2].

The $\langle S^2 \rangle$ expectation values for the triplet states considered (see Table 1) are in every case quite close

to the correct value of 2.0, i.e. spin-contamination is not a problem in our UDFT calculations. Even for the biradicals with an allylic substructure, where the spin-contamination problem should be more pronounced, due to an energetically close-lying quartet state, we find only a slight increase of the $\langle S^2 \rangle$ values to ≈ 2.03 . In this respect, UDFT is clearly superior to unrestricted Hartree–Fock treatments which gives $\langle S^2 \rangle = 2.23$ for BR1, for example.

The double bond twisting path (the reaction coordinate is the dihedral angle C6–C1–C2–C3) has been investigated at CASSCF as well as UDFT theoretical levels. The CASSCF calculations which provide also vertical energies from the lowest singlet state (at the T_1 optimized geometries) are essential here. As expected, the UDFT singlet wavefunctions at large twisting angles suffer from high spin-contamination ($\langle S^2 \rangle = 0.5$ – 0.9). The potential energy curves obtained are shown in Fig. 2. Both theoretical approaches yield flat curves for the T_1 state with a minimum around $\Theta_1 = 10$ – 12 degrees. The energy increases up to $\Theta_1 = 42$ degrees by 13 kcal/mol at the CASSCF level, where the vertical energy difference between the S_0 state (in the T_1 geometry) and the T_1 state becomes zero. The calculated lifetimes of the T_1 state are sensitive to the steepness of the

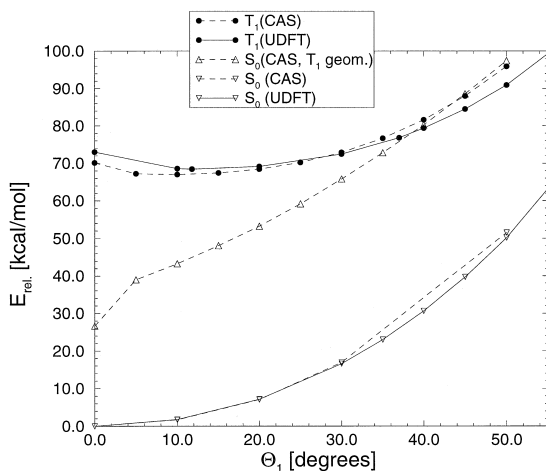


Fig. 2. Potential energy curves (energies in kcal/mol relative to the minimum of the S_0 state) for double bond twisting at CASSCF(2,2) and UDFT–B3LYP levels. The CASSCF energies of the S_0 state have been obtained in single point calculations employing the optimized T_1 geometries (vertical) and also with full S_0 geometry optimization (adiabatic).

Table 2

Calculated spin–orbit matrix elements (in cm^{-1}) between the S_0 and T_1 states for various twisting and syn-pyramidalization angles employing the Breit–Pauli (BP) and effective one-electron spin–orbit (SO) operators at different CASSCF(m,n) levels

Θ / degrees	BP(2,2)	SO(10,10)	SO(2,2)
twisting ^a			
25	0.72	1.53	0.91
30	0.65	1.36	0.82
35	0.56	1.13	0.69
40	0.44	0.87	0.53
pyramidalization ^b			
60	0.87	3.07	0.98
70	0.91	3.19	1.01
80	0.91	3.20	1.01
–60	0.96	3.28	1.03
–70	1.03	3.49	1.12
–80	1.07	3.59	1.17

^a Dihedral angle Θ_1 (C6–C1–C2–C3).

^b Dihedral angle $180 - \Theta_{2/3}$ (H–C1–C2–C3/H–C2–C1–C6).

twisting potential, therefore we have tested the reliability of the CASSCF and UDFT results by comparison with multi-reference singles and doubles configuration interaction calculations (MRD–CI) [12,13]. As expected for states which are dominated by one reference configuration the MRD–CI data are close to the CASSCF and DFT results (UDFT data in parentheses): for the adiabatic S_0 – T_1 excitation energy we obtain 69.5 kcal/mol (68.5) and the energy increase of the T_1 state for 20, 30 and 40 degrees twisting angle is 0.7 (0.6), 4.2 (3.9) and 11.5 (10.9) kcal/mol, respectively.

The calculated SOC matrix elements in the vicinity of the T_1 – S_0 crossing point are given in Table 2. The matrix elements are seen to depend on the active space of the CASSCF wavefunction, in accord with expectations from previous results on ethylene [20], which show that the more accurate SOC values are those corresponding to the large CASSCF active space. For the twist mode, the SOC matrix elements cluster around 0.5–1.5 cm^{-1} , while those for the pyramidalization mode (see below) around 1.0–3.6 cm^{-1} .

A Landau–Zener treatment [21,22] with an excess energy of 13 kcal/mol shows that the probability of crossover is between $P = 5.0 \times 10^{-4}$ (SOC = 0.5 cm^{-1}) and $P = 4.4 \times 10^{-3}$ (SOC = 1.5 cm^{-1}). Us-

ing this probability, an assumed Franck–Condon factor of unity and the rate constant estimated for room temperature ($2.92 \times 10^3 \text{ s}^{-1}$, $A = 10^{13} \text{ s}^{-1}$, $E_a = 13 \text{ kcal/mol}$) we arrive at an upper limit for the total rate of about $1.4\text{--}13.0 \text{ s}^{-1}$ ($\tau = 0.08\text{--}0.69 \text{ s}$). This is much too slow to account for the observed T_1 lifetime of 250 ns [2].

In order to see under which conditions one can obtain a lifetime of the order of the measured value we have also considered the decay of the T_1 state at $\Theta_1 = 30$ degrees where the energy is only 6 kcal/mol higher than in the T_1 minimum. Under the same assumptions ($\text{SOC} = 1.5 \text{ cm}^{-1}$) and ignoring the T_1 – S_0 energy gap entirely the equivalent calculation leads to a rate of deactivation of $1.8 \times 10^6 \text{ s}^{-1}$ ($\tau = 570 \text{ ns}$). However, it should be recalled that the Franck–Condon factors may be much less than unity because of the large geometrical relaxations between S_0 and T_1 and that the assumed preexponential factor A represents really an upper limit for a process involving a torsion motion; furthermore all experience indicates that the calculated relative energy difference between T_1 and S_0 is fairly reliable and that the error is certainly below 5 kcal/mol.

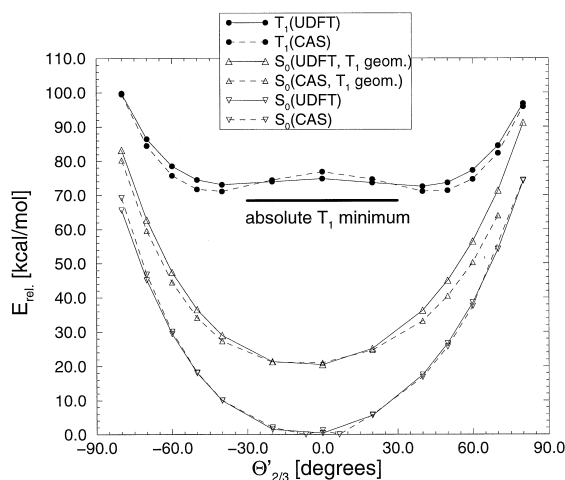


Fig. 3. Potential energy curves (energies in kcal/mol relative to the minimum of the S_0 state) for double bond pyramidalization ($\Theta'_{2/3} = 180 - \Theta_{2/3}$) at CASSCF(2,2) and UDFT–B3LYP levels. The CASSCF energies of the S_0 state have been obtained in single point calculations employing the optimized UDFT–B3LYP geometries of the T_1 (vertical) and S_0 states (adiabatic), respectively. Positive (negative) Θ values indicate pyramidalization towards (opposite to) the bridging CH_2 group.

Finally, we want to show results for the syn-pyramidalization coordinate, prior experience with the SOC in ethene has shown much larger values for the syn- than for the anti-distortion [20]. As expected, the potential energy curves depicted in Fig. 3 along the positive (pyramidalization towards the CH_2 group) and negative pyramidalization coordinates are similar, the latter being slightly lower in energy. As mentioned above, the minima found are about 3–4 kcal/mol higher in energy than the absolute T_1 minimum (see Fig. 1) with a twisted structure. At $|\Theta_{2/3}|$ values larger than 50 degrees the T_1 energy increases steeply. In contrast to what is observed for the curves along the twisting coordinate, we do not locate here a S_0 – T_1 crossing and the singlet-triplet energy gap remains high ($> 10 \text{ kcal/mol}$ up to $|\Theta_{2/3}| = 70$ degrees)¹ Thus, we must conclude that the pyramidalization pathway is associated with an energy barrier too high to afford a fast rate of $T_1 \rightarrow S_0$ decay, irrespective of the SOC value. The calculated SOC values for structures with $180 - |\Theta_{2/3}|$ in the range 60–80 degrees (see Table 2) are only slightly higher (between 1.0 and 3.6 cm^{-1}) than those calculated along the twisting coordinate. It appears therefore, that the only reasonable decay channel occurs in the twisting mode (Fig. 2).

4. Conclusions

We have investigated singlet and triplet energy surfaces for important geometrical distortions and bond breaking pathways in norbornene. Ab initio CASSCF and unrestricted density functional calculations provide similar results not only for the geometries but also for the relative energies of different structures and states. The low spin-contaminations of the UDFT wavefunctions and their low computational cost make them suitable for such studies.

Our investigations of four possible $T_1 \rightarrow S_0$ state

¹ In the UDFT S_0 -state calculations along the pyramidalization coordinate we observed that the wavefunction corresponds essentially to the solution of a restricted DFT calculation. This may explain why the DFT values are higher compared to the CASSCF data at large pyramidalization angles (missing static electron correlation contributions).

deactivation pathways show that the carbon skeleton of norbornene is not so rigid as previously thought. Bond breaking reactions with subsequent intramolecular recombination in the biradical can be excluded for the discussion of the short T_1 state lifetime. The syn-pyramidalization of the double bond also seems not to play an important role in the deactivation process. The most likely decay mechanism involves a moderate twisting of the norbornene skeleton accompanied by opposite motions of the vinylic hydrogens. In this case, a S_0 – T_1 surface crossing occurs, but the calculated energy at the crossing point relative to the T_1 state minimum is too high to account for the observed fast rate of decay. It appears therefore that calculations of the isolated molecule cannot account for the short T_1 lifetime measured in benzene solution [2].

Acknowledgements

This research is supported by a grant to SS and SDP (I-461-230.5/95) from the G.I.F (German–Israeli Foundation). The services and computer time made available by the Sonderforschungsbereich 334 (‘Wechselwirkungen in Molekülen’) have been essential to this study.

References

- [1] N.J. Turro, *Modern Molecular Photochemistry*, Benjamin Cummings, Menlo Park, 1978.
- [2] A.J.G. Barwise, A.A. Gorman, M.A.J. Rodgers, *Chem. Phys. Lett.* 38 (1976) 313.
- [3] H.E. Zimmerman, K.S. Kamm, D.P. Werthemann, *J. Am. Chem. Soc.* 97 (1975) 3718.
- [4] MOLPRO (Vers. 94.10) is a package of ab initio programs written by H.-J. Werner, P.J. Knowles with contributions from J. Almlöf, R.D. Amos, M.J.O. Deegan, S.T. Elbert, C. Hample, W. Meyer, K. Peterson, R. Pitzer, A.J. Stone, P.R. Taylor.
- [5] R. Ahlrichs, M. Bär, M. Häser, H. Horn, C. Kölmel, *Chem. Phys. Lett.* 162 (1989) 165.
- [6] O. Treutler, R. Ahlrichs, *J. Chem. Phys.* 102 (1995) 346.
- [7] A.D. Becke, *J. Chem. Phys.* 98 (1993) 5648.
- [8] P.J. Stephens, F.J. Devlin, C.F. Chabalowski, M.J. Frisch, *J. Phys. Chem.* 98 (1994) 11623.
- [9] A. Schäfer, H. Horn, R. Ahlrichs, *J. Chem. Phys.* 97 (1992) 2571.
- [10] J. Baker, *J. Comp. Chem.* 7 (1986) 385.
- [11] J.J.P. Stewart, *J. Comp. Chem.* 10 (1989) 209.
- [12] R.J. Buenker, S.D. Peyerimhoff, *Theor. Chim. Acta* 35 (1974) 33.
- [13] R.J. Buenker, S.D. Peyerimhoff, *Theor. Chim. Acta* 39 (1975) 217.
- [14] M. Hanrath, B. Engels, *Chem. Phys.* 225 (1997) 197.
- [15] S.R. Langhoff, E.R. Davidson, *Int. J. Quant. Chem.* 81 (1974) 61.
- [16] GAMESS-USA (Rev. Mar. 1997): M.W. Schmidt, K.K. Baldridge, J.A. Boatz, S.T. Elbert, M.S. Gordon, J.H. Jensen, S. Koseki, N. Matsunaga, K.A. Nguyen, S.J. Su, T.L. Windus, M. Dupuis, J.A. Montgomery; see e.g. *J. Comp. Chem.* 14 (1993) 1347.
- [17] S. Koseki, M.W. Schmidt, M.S. Gordon, *J. Phys. Chem.* 96 (1992) 10768.
- [18] S. Koseki, M.S. Gordon, M.W. Schmidt, N. Matsunaga, *J. Phys. Chem.* 99 (1995) 12764.
- [19] R.J. Buenker, S.D. Peyerimhoff, *Chem. Phys.* 9 (1976) 75.
- [20] D. Danovich, C.M. Marian, T. Neuheuser, S.D. Peyerimhoff, S. Shaik, *J. Phys. Chem.*, submitted.
- [21] L.D. Landau, *Phys. Z. Sowjetunion* 2 (1932) 46.
- [22] C. Zener, *Proc. R. Soc. London Ser. AB* 7 (1932) 696.